

Article

Sulfonated Binaphthyl-Containing Poly(arylene ether ketone)s with Rigid Backbone and Excellent Film-Forming Capability for Proton Exchange Membranes

Wenmeng Zhang ¹, Shaoyun Chen ², Dongyang Chen ^{1,*}  and Zhuoliang Ye ^{3,*}

¹ College of Materials Science and Engineering, Fuzhou University, Fuzhou 350116, China; wenmeng_zhang@163.com

² College of Chemical Engineering and Materials Science, Quanzhou Normal University, Quanzhou 362000, China; aassdd_ff123@126.com

³ College of Chemical Engineering, Fuzhou University, Fuzhou 350116, China

* Correspondence: dongyang.chen@fzu.edu.cn (D.C.); ye_zhuoliang@163.com (Z.Y.); Tel.: +86-182-5019-9000 (D.C.)

Received: 26 October 2018; Accepted: 16 November 2018; Published: 19 November 2018



Abstract: Sterically hindered (S)-1,1'-binaphthyl-2,2'-diol had been successfully copolymerized with 4,4'-sulfonyldiphenol and 4,4'-difluorobenzophenone to yield fibrous poly(arylene ether ketone)s (PAEKs) containing various amounts of binaphthyl unit, which was then selectively and efficiently sulfonated using ClSO₃H to yield sulfonated poly(arylene ether ketone)s (SPAEEKs) with ion exchange capacities (IECs) ranging from 1.40 to 1.89 mmol·g⁻¹. The chemical structures of the polymers were confirmed by 2D ¹H-¹H COSY NMR and FT-IR. The thermal properties, water uptake, swelling ratio, proton conductivity, oxidative stability and mechanical properties of SPAEEKs were investigated in detail. It was found that the conjugated but non-coplanar structure of binaphthyl unit endorsed excellent solubility and film-forming capability to SPAEEKs. The SPAEK-50 with an IEC of 1.89 mmol·g⁻¹ exhibited a proton conductivity of 102 mS·cm⁻¹ at 30 °C, much higher than that of the state-of-the-art Nafion N212 membrane and those of many previously reported aromatic analogs, which may be attributed to the likely large intrinsic free volume of SPAEEKs created by the highly twisted chain structures and the desirable microscopic morphology. Along with the remarkable water affinity, thermal stabilities and mechanical properties, the SPAEEKs were demonstrated to be promising proton exchange membrane (PEM) candidates for potential membrane separations.

Keywords: proton exchange membranes; condensation polymerization; post-sulfonation; binaphthyl; film-forming capability

1. Introduction

Proton exchange membranes (PEMs) have attracted more and more attention as separators for electrodialysis, electrolysis, pervaporation, fuel cells and flow batteries [1–4]. The key function of PEMs is to efficiently and selectively conduct certain mass while blocking the permeation of the others. The state-of-the-art PEM is Nafion, which is a perfluorosulfonic acid ionomer with outstanding proton conductivity and excellent chemical stability. However, it suffers from several drawbacks such as severe fuel permeation and high cost [5]. Therefore, lots of works have been devoted to the development of alternative PEMs, including sulfonated polystyrenes [6–8], sulfonated poly(arylene ether)s [9–12], sulfonated poly(arylene thioether)s [13,14], sulfonated poly(ether amide)s [15], sulfonated polyimides [16,17], sulfonated polybenzimidazoles [18], and sulfonated poly(phthalazinone

ether)s [19,20]. Among them, sulfonated poly(arylene ether)s have been widely researched because of their good film-forming capability, robust mechanical strength, high thermal stability, and tunable proton conductivity [3,5].

During the design of high performance sulfonated poly(arylene ether)s, the position of sulfonic acid group along the poly(arylene ether) backbones is an important parameter, because it not only affects the thermal and chemical stability of the resultant polymer, but also the micro-morphology and proton conductivity of the final membrane [21–23]. The polymers with sulfonic acid group tethering at the pendant chains are reported to be more stable against hydrolysis and thermal decomposition than those with sulfonic acid group tethering directly at the backbone of the polymers [24,25]. Moreover, pendant sulfonic acid groups are more likely to form ionic aggregates than backbone sulfonic acid groups, thus leading to faster proton conduction [26]. Currently, lots of studies have been devoted to the synthesis of ionomers with ion clustering structures for highly proton conductive membranes [3,27]. Many strategies have been proposed, such as the design of hydrophilic-hydrophobic multi-block structures from multi-step reactions [28,29] and the design of densely sulfonated structures from monomers containing several reactive sites [30,31]. For example, Matsumura et al. developed a phenol molecule with 6 electron-rich phenyl rings, which after incorporation to the end of polymer chains and sulfonation in succession yielded densely sulfonated PEM with a high proton conductivity of $6.9 \text{ mS}\cdot\text{cm}^{-1}$ at a low IEC of $0.48 \text{ mmol}\cdot\text{g}^{-1}$ [32]. Similarly, Matsumoto et al. developed a bisphenol monomer with 8 electron-rich phenyl rings, which after polymerization and sulfonation yielded densely sulfonated PEMs with similar proton conductivity to Nafion at an IEC of $1.77 \text{ mmol}\cdot\text{g}^{-1}$ [30]. In addition, Bae et al. synthesized sulfonated poly(arylene ether sulfone ketone) multiblock copolymers with a highly sulfonated block, and achieved comparable proton conductivity to Nafion at an IEC of $1.86 \text{ mmol}\cdot\text{g}^{-1}$ [33]. While enhanced proton conductivity can be achieved, these strategies usually involve complex reactions which require sophisticated experimental skills and add up to the cost of the products. Also, the scaling up of the synthesis of many well-designed monomers is still unknown. Therefore, there is still a need to develop high performance PEMs from commercially available compounds using few reaction steps.

1,1'-Binaphthyl-2,2'-diol is a chiral organic compound that is often used as a ligand for transition-metal catalyzed asymmetric synthesis [34,35]. Unlike traditional high-activity bisphenol monomers that have been used for condensation polymerization to make poly(arylene ether)s, the rigid 1,1'-binaphthyl-2,2'-diol has a pair of phenol groups facing to each other within a short spacing, yielding high steric hindrance for the complete $\text{S}_{\text{N}}2$ substitution of the phenol groups. Herein, we report our effort to polymerize 1,1'-binaphthyl-2,2'-diol with activated aromatic dihalide to achieve mechanically robust poly(arylene ether ketone)s, which is then sulfonated at the binaphthyl unit to introduce the sulfonic acid groups. The chemical structure of the products and their physicochemical properties are investigated in detail. It is demonstrated that these binaphthyl-containing ionomers are promising PEM candidates for potential membrane separations.

2. Materials and Methods

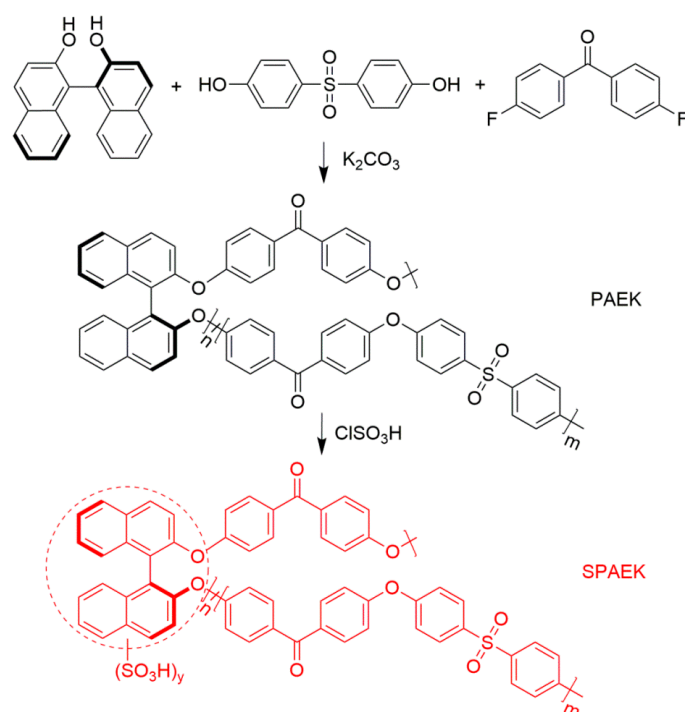
2.1. Materials

(S)-1,1'-binaphthyl-2,2'-diol, 4,4'-difluorobenzophenone, 4,4'-sulfonyldiphenol, ethanol, methanol, dichloromethane, chlorosulfonic acid, toluene, *N,N*-dimethylacetamide (DMAc), anhydrous potassium carbonate, sulfuric acid, sodium hydroxide, sodium sulfate were purchased from Aladdin Co, Shanghai, China. (S)-1,1'-binaphthyl-2,2'-diol and 4,4'-sulfonyldiphenol were vacuum dried at $80 \text{ }^{\circ}\text{C}$ for 12 h. 4,4'-difluorobenzophenone was recrystallized from ethanol. Other chemicals were used as received.

2.2. Synthesis of Poly(arylene ether ketone)s (PAEKs)

(S)-1,1'-binaphthyl-2,2'-diol was copolymerized with 4,4'-sulfonyldiphenol and 4,4'-difluoro benzophenone using a traditional condensation polymerization protocol, as depicted in Scheme 1.

The feeding ratios of (S)-1,1'-binaphthyl-2,2'-diol in the bisphenol monomers were 35%, 43%, and 50%, which yields PAEK-35, PAEK-43, and PAEK-50 as product, respectively. The typical synthesis of PAEK-50 was described as followed. To a 25 mL three-necked round-bottom flask equipped with a magnetic stirrer, a thermometer, a dean-stark trap, a condenser, an Ar inlet and an Ar outlet, 0.5727 g (2 mmol) of (S)-1,1'-binaphthyl-2,2'-diol, 0.5005 g (2 mmol) of 4,4'-sulfonyldiphenol, 0.8728 g (4 mmol) of 4,4'-difluorobenzophenone, 0.83 g (6 mmol) of potassium carbonate, 14 mL of DMAc and 8 mL of toluene were introduced carefully. Firstly, the reaction mixture was heated at 140–145 °C for 3 h, during which the produced water was removed by azeotropic distillation with toluene. Secondly, the toluene and water in the dean-stark trap were removed, and the excess toluene in the reaction mixture was distilled into the dean-stark trap. After that, the reaction mixture was heated to 160–165 °C and maintained at that temperature for 16 h. Upon cooling down to ~80 °C, the resulting viscous mixture was poured into 300 mL of deionized water to form fibrous product. The product was collected by filtration, purified by re-dissolving in dichloromethane and precipitating in methanol. The final product was dried under vacuum at 80 °C for 24 h.



Scheme 1. Copolymerization of (S)-1,1'-binaphthyl-2,2'-diol with electron-deficient monomers and the subsequent sulfonation process.

2.3. Sulfonation of PAEKs

The PAEKs were sulfonated by chlorosulfonic acid, as also shown in Scheme 1. The feeding ratio of chlorosulfonic acid to binaphthyl unit was 10:1. The typical synthesis of SPAEK-50 was described as followed. To a 500 mL three-necked round-bottom flask equipped with a magnetic stirrer, an addition funnel, an Ar inlet and an Ar outlet, 1 g (2.37 mmol) of PAEK-50 and 300 mL of anhydrous dichloromethane were charged. After the PAEK-50 was dissolved completely in dichloromethane, 23.7 mL of 1 M chlorosulfonic acid in dichloromethane was added drop-wise into the reaction mixture through the addition funnel. The reaction mixture was vigorously stirred for 12 h. Brown solid product was formed and segregated at bottom of the flask during the course. Then the dichloromethane was poured out directly, and fresh dichloromethane was added to wash out the chlorosulfonic acid residue. After that, 20 mL of DMAc was added to dissolve the brown solid product, and 0.4 M of NaOH aqueous solution was added drop-wise through an addition funnel to neutralize the solution. Finally,

the polymer solution was dialyzed for 3 days using a dialysis membrane (cut-off molecular weight: 4000 Da). The product SPAEK-50 was obtained by evaporating the water.

2.4. Membrane Preparation

SPAEEKs were dissolved in DMAc with a concentration of 8% (wt/vol.). The polymer solutions were filtered and cast onto leveled glass plates conditioning in an oven with an exhaust vent. After being dried at 80 °C for 12 h, the glass plates were transferred into a vacuum oven and dried at 80 °C for another 12 h. Polymer membranes were formed on the glass plates. The membranes were peeled off the glass plates, immersed in 1 M H₂SO₄ aqueous solution at 80 °C for 1 h, immersed in deionized water at 80 °C for 1 h, and stored in deionized water until use.

2.5. Characterizations

¹H nuclear magnetic resonance (NMR) spectrum was recorded using a Bruker AVANCE III 500 nuclear magnetic resonance spectrometer (Bruker Corporation, Karlsruhe, Germany), and the chemical shifts were listed in parts per million (ppm) downfield from tetramethylsilane. FT-IR of polymer films was measured by a ThermoFisher Nicolet 5700 Fourier infrared spectrometer (Thermo Fisher Scientific, Waltham, MA, USA). Differential scanning calorimetry (DSC) was tested by a NETZSCH DSC 214 Polyma instrument (NETZSCH, Selb, Germany), with samples being heated from 50 to 300 °C, cooled down to 50 °C, and then heated to 300 °C again at a temperature rate of 10 °C·min⁻¹. The second heating process was recorded. Thermogravimetric analysis (TGA) was carried out using a TA SDT Q600 instrument (TA Instruments, New castle, DE, USA) with samples being hold at 180 °C for 15 min to remove the residual solvents and then heated to 600 °C at a heating rate of 10 °C·min⁻¹. The stress-strain curves were recorded by a SANS Electronic Universal Testing Station (SUNS Technology, Shenzhen, China) with a crosshead speed of 5 mm·min⁻¹. Membrane samples were cut into a size of 50 mm × 5 mm. The measurements were carried out at room temperature (28 °C) and environmental humidity (79% RH). Gel permeation chromatography (GPC) analysis was performed on a Waters Breeze system equipped with a Waters Styragel column (Waters Corporation, Milford, MA, USA), Waters 515 HPLC pump, and Waters 2414 refractive index detector, tetrahydrofuran as the elution solvent at a flow rate of 1 mL·min⁻¹ and polystyrene as standards for calibration. Small angle X-ray scattering (SAXS) was tested by an Anton Paar SAXSess mc² instrument (Anton Paar GmbH, Graz, Austria).

The inherent viscosity (η) of sulfonated polymers was measured by an ubbelohde viscometer at 30 °C, with the solvent of NMP containing 0.05 M of LiBr. The η was calculated by Equation (1):

$$\eta = (t - t_0) / t_0 \times C_0 \quad (1)$$

where t is the outflow time of the polymer solution, t_0 is outflow time of the solvent, C_0 (0.5 g·dL⁻¹) is the mass concentration of the polymer. The test was repeated for three times and the average value was taken.

The ionic exchange capacity (IEC) of the SPAEEKs was determined by acid-base titration. The membrane samples were immersed in 2 M Na₂SO₄ aqueous solution for 24 h to exchange the H⁺ of the samples into the solution. The exchanged H⁺ was titrated by 0.1 M NaOH aqueous solution with phenolphthalein as indicator. The IEC_{titrated} was calculated by Equation (2):

$$IEC_{titrated} = (\Delta V \times C) / W_d \quad (2)$$

where ΔV is the consumed volume of NaOH solution, C is the concentration of NaOH solution, and W_d is the weight of the dry membrane.

The sulfonation degree (SD) was calculated by Equation (3):

$$SD = IEC_{titrated} / IEC_{theoretical} \times 100\% \quad (3)$$

where $IEC_{theoretical}$ is the theoretical IEC of the polymers calculated based on the full sulfonation of binaphthyl unit with two sulfonic acid groups.

The water uptake and swelling ratio of the membranes at specific conditions were defined as their weight and length change to those of the dry membranes, and were calculated by Equations (4) and (5) respectively:

$$\text{Water uptake} = (W_w - W_d)/W_d \times 100\% \quad (4)$$

$$\text{Swelling ratio} = (L_w - L_d)/L_d \times 100\% \quad (5)$$

where W_w and W_d are the weight of the wet and dry membrane, respectively; L_w and L_d are the length of the wet and dry membrane, respectively.

Oxidative stability of the membranes was evaluated by immersing the samples in Fenton's reagent (3 wt % H_2O_2 + 2 ppm $FeSO_4$) at 80 °C with constant shaking. The time for each sample starting to break was recorded.

The in-plane proton conductivity of the membranes was determined by electrochemical impedance spectroscopy (EIS) using a Solartron 1287 electrochemical interface with the frequency range of 10 MHz to 1 Hz. The proton conductivity (σ) was calculated by Equation (6):

$$\sigma = d/RS \quad (6)$$

where d and S are the thickness and area of the membrane, respectively; R is the membranes' resistance derived from the EIS curve.

3. Results and Discussion

3.1. Polymerization

Commercially available poly(arylene ether)s are usually synthesized from condensation polymerization of bisphenol compounds with activated dihalide compounds. The widely used bisphenol compounds include bisphenol A, bisphenol F, bisphenol AF, and 4,4'-biphenol, all of which contains sterically unhindered phenolic hydroxyl group. It has been reported that the methyl-hindered phenolic hydroxyl group needs extended reaction time for the complete reaction to achieve considerable molecular weight of the product [36]. Therefore, it is challenging to synthesize poly(arylene ether)s from sterically hindered (S)-1,1'-binaphthyl-2,2'-diol. We started the polymerization of (S)-1,1'-binaphthyl-2,2'-diol with a stoichiometric amount of 4,4'-difluoro benzophenone or 4,4'-difluorophenylsulfone in the presence of K_2CO_3 in DMAc at 160 °C. The produced water was removed before polymerization by azeotropic distillation with toluene. After polymerizing for 2 days, only small molecular weight products were obtained, which couldn't be cast into free-standing membranes. Therefore, we had to use a sterically unhindered bisphenol compound, bisphenol S, to copolymerize with (S)-1,1'-binaphthyl-2,2'-diol. The selection of bisphenol S, rather than bisphenol A or the others, was because of its electron-deficient phenyl ring that would remain stable in the forthcoming post-sulfonation process.

It was found that when the loading amount of (S)-1,1'-binaphthyl-2,2'-diol was higher than 50% of the total bisphenol loading, only oligomers were resulted. By reducing the amount of (S)-1,1'-binaphthyl-2,2'-diol to 50%, 43% and 35%, fibrous products of PAEK-50 (Figure 1a), PAEK-43, and PAEK-35 were obtained after a reaction time of 24 h. The products were highly soluble in chloroform, dichloromethane, DMAc, NMP, and DMF, probably due to the conjugated but non-coplanar structure of the binaphthyl unit that decreased the packing order of the polymer chains and thus increased the solubility of the polymers, which is similar to an experimental observation that was reported for poly(phthalazinone ether)s [37]. The chemical structures of PAEKs were confirmed by 2D 1H - 1H COSY NMR spectrum, as shown in Figure 2. The resonance peaks for all of the polymer segments are well assigned, suggesting the successful incorporation of binaphthyl unit into the polymers. The number-average molecular weights of PAEKs were found to be higher than 35 kDa

by GPC characterizations, as listed in Table 1. Such high molecular weights of PAEKs suggest their promising application as scaffolds for free-standing membranes.

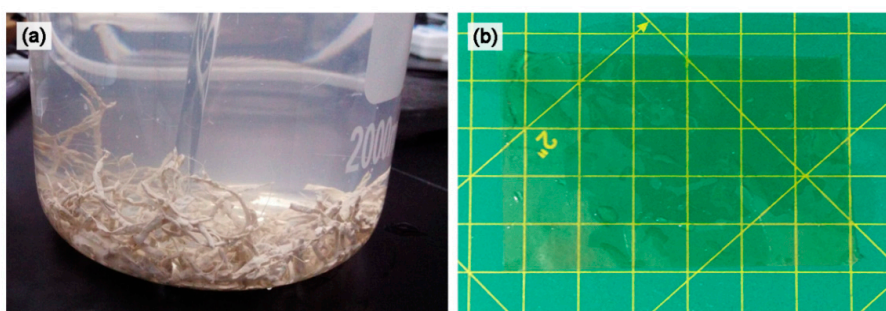


Figure 1. (a) Digital photo of fibrous PAEK-50 precipitated in water; (b) digital photo of a transparent SPAEK-50 membrane.

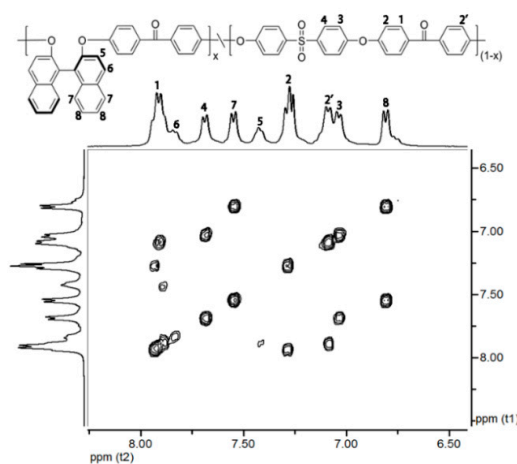


Figure 2. 2D ^1H - ^1H COSY NMR spectrum of PAEK-50 in CDCl_3 .

Table 1. Average molecular weights and polydispersity index of PAEKs.

Sample	Mn (kDa)	Mw (kDa)	Polydispersity Index
PAEK-35	42	67	1.6
PEAK-43	35	58	1.7
PAEK-50	51	76	1.5

The thermal properties of PAEKs were investigated by DSC and TGA under a protective nitrogen atmosphere. As can be seen from Figure 3a, all of the three PAEKs exhibit only one glass transition in the temperature range from 120 to 300 °C, typical phenomenon of random poly(arylene ether)s. The glass transition temperatures (T_g) for PAEK-35, PAEK-43 and PAEK-50 are 198 °C, 203 °C and 210 °C, respectively. The increasing T_g agrees well with the increasing content of the rigid binaphthyl unit in the polymers, suggesting that the binaphthyl unit attributed to the enhanced thermal properties of PAEKs. It is worth mentioning that the T_g values of PAEKs are higher than those of many well-studied poly(arylene ether)s in literature [31,38], suggesting the promising prospect of PAEKs for high performance engineering plastics. The initial thermal decomposition temperatures of PAEKs are all around 400 °C, as shown in Figure 3b. Only one decomposition step can be observed, with 5% weight-loss decomposition temperature being 424.5 °C, 431.4 °C, and 444.5 °C for PAEK-35, PAEK-43, and PAEK-50, respectively. The higher the binaphthyl content in the polymer, the higher the thermal decomposition temperature. Therefore, the incorporation of binaphthyl unit elevates not only the glass transition temperature but also the thermal decomposition temperature of the products.

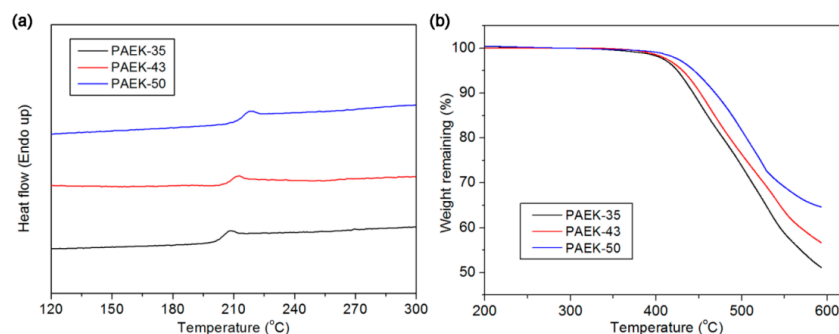


Figure 3. (a) DSC and (b) TGA curves of PAEKs.

3.2. Sulfonation

Sulfonation of PAEKs was carried out at room temperature using ClSO_3H as sulfonation agent and CH_2Cl_2 as solvent. The ClSO_3H was diluted with CH_2Cl_2 firstly and added into the reaction mixture drop by drop to ensure the reactions taking place at the desired positions and with high yield. The sulfonated products SPAEKs are highly soluble in polar aprotic solvents such as DMAc, DMF, DMSO, and NMP, but nearly insoluble in low polar solvents such as CH_2Cl_2 and CHCl_3 . The high solubility of SPAEKs in polar aprotic solvents may be due to the conjugated but non-coplanar structure of binaphthyl unit, similar to an experimental observation that was reported for sulfonated poly(phthalazinone ether)s [19,20]. The inherent viscosity of all of the SPAEKs were about $0.4 \text{ dL}\cdot\text{g}^{-1}$, regardless of the different amounts of (S)-1,1'-binaphthyl-2,2'-diol used in the polymerization.

The chemical structures of SPAEKs were characterized by 2D ^1H - ^1H COSY NMR, as shown in Figure 4. The resonance peaks 1 and 2 for the benzophenone segment and the resonance peaks 3 and 4 for the bisphenol S segment can be well assigned based on their chemical shifts and integral values, plus the reference from the ^1H NMR of PAEKs (Figure 2). Before sulfonation, the aromatic protons near the ketone and sulfone groups are the most electron-deficient protons on the polymer backbones, with resonance peaks 1 and 2 showing up at the low magnetic field of ^1H NMR spectra. After sulfonation, two resonance peaks arise at the lower magnetic field than peaks 1 and 2, suggesting the existence of even more electron-deficient protons than the protons near the ketone and sulfone groups on the polymer backbone—an indication of the successful introduction of electron-withdrawing groups, namely sulfonic acid groups. Since the sulfonic acid groups can be introduced to different positions of the binaphthyl unit to add up the complexity of the ^1H NMR spectrum, it is hard to assign all the peaks of SPAEKs as in the case of pure and small organic molecules.

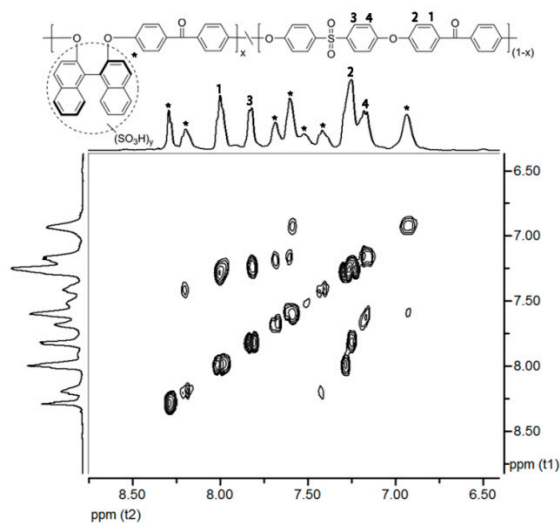


Figure 4. 2D ^1H - ^1H COSY NMR spectrum of SPAEK-50 in DMSO-d_6 .

To further verify the introduction of sulfonic acid group to PAEKs, representative FT-IR spectra of PAEK-35 and SPAEK-35 were recorded, as shown in Figure 5. Both samples exhibit absorption peaks of C=O at 1653 cm^{-1} , C=C at 1585 cm^{-1} and Ph-O-Ph at 1243 cm^{-1} , in keeping with the poly(arylene ether ketone) backbone structure. Compared to the FT-IR spectrum of PAEK-35 (without sulfonic acid groups), there is a new absorption peak at 1036 cm^{-1} in the FT-IR spectrum of SPAEK-35, which can be attributed to the vibration of O=S=O from the sulfonic acid groups [38]. Therefore, both the ^1H NMR and FT-IR results validate the successful introduction of sulfonic acid groups to the PAEKs.

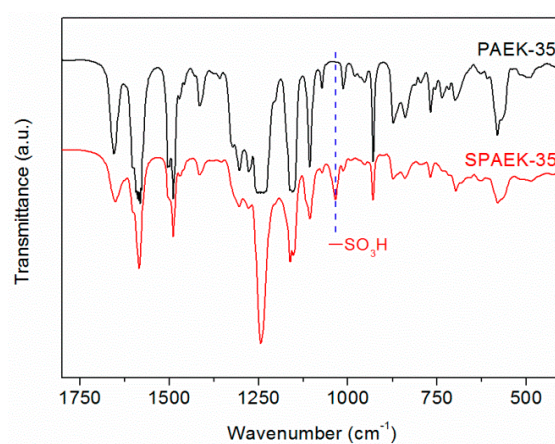


Figure 5. FT-IR spectra of PAEK-35 and SPAEK-35.

3.3. Ion Exchange Capacity of SPAEKs

Flexible SPAEK membranes (Figure 1b) were obtained by a solution-casting method. The ion exchange capacities (IECs) of the membranes were titrated and listed in Table 2 along with the theoretical IECs. It can be seen that both the theoretical and titrated IECs increase with the increasing content of binaphthyl unit in the polymers. The titrated IECs for SPAEK-35, SPAEK-43, and SPAEK-50 were 1.25 , 1.63 , and $1.82\text{ mmol}\cdot\text{g}^{-1}$, respectively, corresponding to the sulfonation degree of 89%, 99%, and 96%, respectively. Therefore, it can be concluded that ClSO_3H is a satisfying sulfonation agent for PAEKs, and the resulting IEC can be easily tuned by the molar content of binaphthyl unit in the PAEK backbone.

Table 2. IEC, SD and oxidative stability of SPAEKs.

Sample	Theoretical IEC (mmol g^{-1})	Titrated IEC (mmol g^{-1})	SD (%)	Oxidative Stability (min.)
SPAEK-35	1.40	1.25	89	80
SPAEK-43	1.65	1.63	99	75
SPAEK-50	1.89	1.82	96	65

3.4. Water Affinity and Proton Conductivity of SPAEKs

Water is essentially important for the dissociation and conduction of protons. The water uptake and swelling ratio of SPAEKs were measured at four different temperatures, as shown in Figure 6a,b. It can be seen that both the water uptake and swelling ratio of SPAEKs increase with the increasing IEC and the increasing temperature, as expected. The water uptake of SPAEK-35 is 26.6% at $30\text{ }^\circ\text{C}$, while that of SPAEK-50 is 49.1% at the same temperature. For comparison, Nafion N212 shows a water uptake of 19.8% at $30\text{ }^\circ\text{C}$, slightly lower than that of SPAEK-35. Similarly, the swelling ratio of Nafion N212 (7.4% at $30\text{ }^\circ\text{C}$) is also slightly lower than that of SPAEK-35 (8.3% at $30\text{ }^\circ\text{C}$). All of the SPAEKs exhibit moderate water uptake and swelling ratio, suggesting the promising prospect for PEM applications.

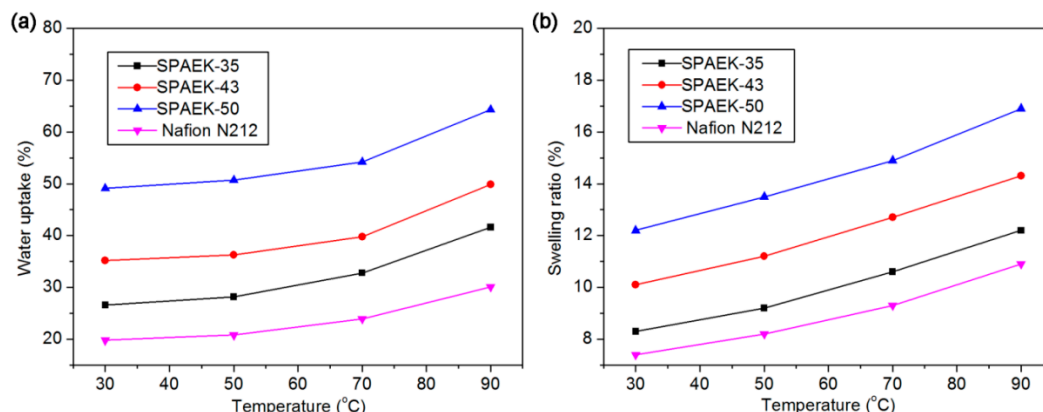


Figure 6. (a) Water uptake and (b) swelling ratio of SPAEKs and Nafion N212 as a function of temperature.

As one of the most important parameters for PEMs, the proton conductivity of SPAEKs was also investigated at four different temperatures, as shown in Figure 7a. It can be seen that the proton conductivities of SPAEKs increase with the increasing IEC at any given temperature, which can be attributed to the higher amount of proton and water for samples with higher IECs. Besides, the proton conductivity of SPAEKs also increase with the increasing temperature, which can be attributed to the higher amount of water and energy for the conduction of proton at higher temperatures. Encouragingly, the SPAEK-50 with an IEC of $1.89 \text{ mmol}\cdot\text{g}^{-1}$ exhibit a proton conductivity of $102 \text{ mS}\cdot\text{cm}^{-1}$ at $30 \text{ }^\circ\text{C}$, much higher than that of the state-of-the-art Nafion N212 membrane, which is only $87 \text{ mS}\cdot\text{cm}^{-1}$. Generally, the proton conductivities of randomly sulfonated polymers are relatively low even at high IECs because of the lack of effective proton conduction path [38,39]. The proton conductivities of SPAEKs are higher than those of other randomly sulfonated analogs at similar IECs (sPTPOF-100 [13], IEC = $1.32 \text{ mmol}\cdot\text{g}^{-1}$, $\sigma = 43 \text{ mS}\cdot\text{cm}^{-1}$; SPTKK [14], IEC = $1.91 \text{ mmol}\cdot\text{g}^{-1}$, $\sigma = 13.6 \text{ mS}\cdot\text{cm}^{-1}$; **2b-3** [36], IEC = $1.67 \text{ mmol}\cdot\text{g}^{-1}$, $\sigma = 17.0 \text{ mS}\cdot\text{cm}^{-1}$), which may be attributed to the likely large intrinsic free volume of the membranes created by the highly twisted chain structures, a phenomenon that had recently been demonstrated in a similar system containing sterically hindered triptycene moiety [40]. The Arrhenius activation energy (E_a) for proton conduction can be calculated from the slope of the linear fit of $\ln \sigma$ vs. $1/T$ (Figure 7b) through $\ln \sigma = \ln \sigma_0 - E_a/RT$, where σ is the proton conductivity, σ_0 is the pre-exponential factor, R is the gas constant, and T is the absolute temperature. The calculated E_a values for the SPAEK-35, SPAEK-43, and SPAEK-50 are 21.6, 21.2, and 21.7 $\text{kJ}\cdot\text{mol}^{-1}$, respectively, which are comparable to that of Nafion N212 ($20.6 \text{ kJ}\cdot\text{mol}^{-1}$).

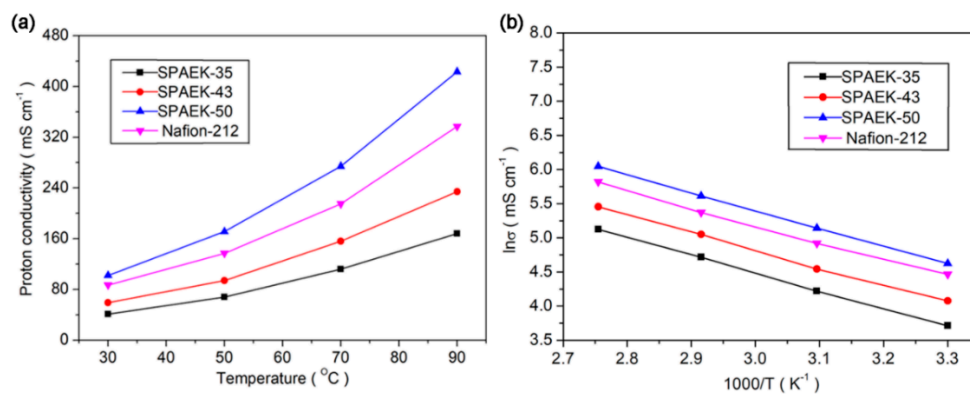


Figure 7. Proton conductivity of SPAEKs and Nafion N212 as a function of temperature.

3.5. Thermal Stability and Oxidative Stability of SPAEKs

The thermal stability of SPAEKs was investigated by TGA, as shown in Figure 8. It can be seen that there are two weight-loss stages for SPAEKs, similar to those of other sulfonated analogs in literature [26,31]. The first stage at ~240–400 °C can be attributed to the elimination of the sulfonic acid groups, while the second stage at ~500–600 °C can be attributed to the decomposition of the aromatic backbones. The initial thermal decomposition temperature of SPAEKs shows minor dependence on the IEC. All of the initial decomposition temperatures of SPAEKs are higher than 200 °C, suggesting good thermal stability for the application in low-medium temperature devices.

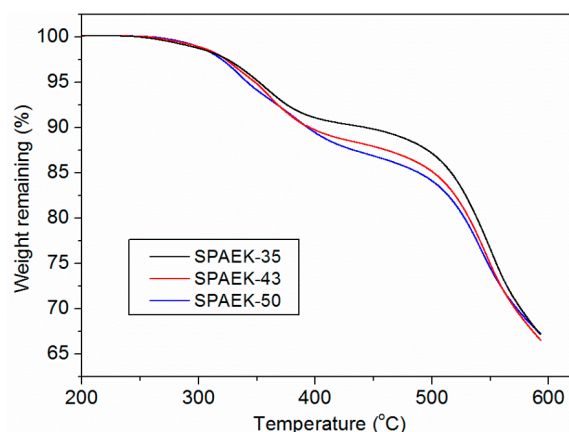


Figure 8. TGA curves of SPAEKs.

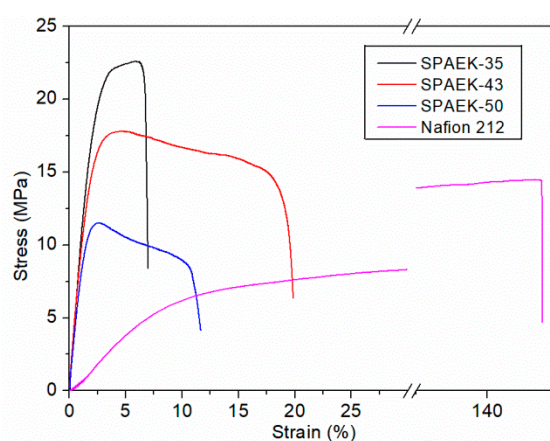
The oxidative stabilities of SPAEKs were evaluated by emerging the membranes in Fenton's reagent at 80 °C, as listed in Table 2. It can be seen that the SPAEK-35 has the highest oxidative stability, while the SPAEK-50 has the lowest oxidative stability. Such variation in oxidative stability can be attributed to the variation in water uptake which carries the oxidative species into the membranes to initiate the degradation. The oxidative stabilities of SPAEKs are comparable to those of other non-fluorinated analogs in literature [38], and are inferior to those of fluorinated PEMs [41]. Therefore, the incorporation of F atom into SPAEKs is anticipated to further improve their oxidative stabilities.

3.6. Mechanical Properties of SPAEKs

The mechanical properties of SPAEKs were measured at room temperature under ambient relative humidity (RH, 79%). Since water acts as plasticizer in the membrane, the water uptake and swelling ratio of the samples have also been recorded under the same condition. It can be seen from Table 3 that the water uptake and swelling ratio of samples recorded under ambient RH are lower than those recorded under 100% RH (Figure 6a), as expected. The stress-strain curves of SPAEKs were shown in Figure 9 with the corresponding tensile strength and elongation at break values listed in Table 3. It can be seen that the SPAEK-35 with the lowest water uptake shows the highest tensile strength of 22.6 MPa, while the SPAEK-50 with the highest water uptake of 12.6% shows the lowest tensile strength of 11.5 MPa. For comparison, Nafion N212 shows a tensile strength of 15.9% under the same condition, which is slightly higher than that of the SPAEK-50 but lower than those of SPAEK-35 and SPAEK-43. The elongations at break of SPAEKs are much lower than that of Nafion N212 because of the presence of rigid aromatic backbones. The trend of elongation at break of SPAEKs is not clear probably because of its high sensitivity toward microscopic defects formed during the sample preparation process.

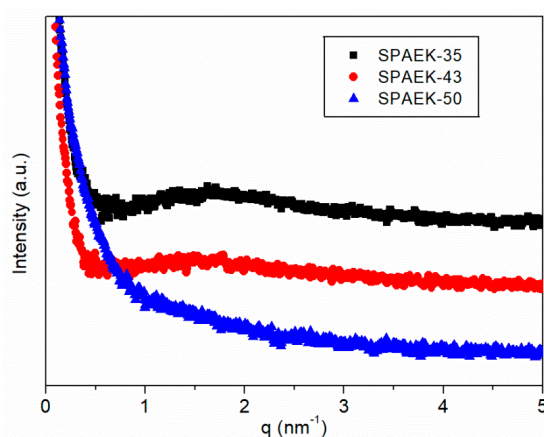
Table 3. Water affinity and mechanical property of SPAEKs and Nafion N212 under ambient RH.

Sample	Water Uptake (wt %)	Swelling Ratio (%)	Tensile Strength (MPa)	Elongation at Break (%)
SPAEK-35	10.9	3.4	22.6	6.9
SPAEK-43	12.3	4.2	17.8	19.9
SPAEK-50	12.6	5.9	11.5	11.6
N212	7.2	4.7	15.9	374.1

**Figure 9.** Tensile properties of SPAEKs under ambient RH.

3.7. Microscopic Morphologies of SPAEKs

The microscopic morphologies of SPAEKs were investigated by small angle X-ray scattering (SAXS) technique, as shown in Figure 10. The separation of hydrophilic and hydrophobic segments of PEMs usually produces an ionomer peak in SAXS profiles, which is attributed to the electron density difference between the two domains. An obvious ionomer peak at the q of 1.65 nm^{-1} can be found for SPAEK-35, corresponding to an inter-domain spacing of 3.8 nm. The peak intensity decreases with the increase in IEC, presumably because of the increased phase mixing and shorter non-ionic segment length in high IEC samples [42]. The desirable morphology of SPAEKs may be another reason for its superior proton conductivities.

**Figure 10.** SAXS profiles of SPAEKs.

4. Conclusions

Sulfonated poly(arylene ether ketone)s (SPAEEKs) containing sterically hindered binaphthyl unit had been successfully synthesized with high molecular weights from the (i) condensation polymerization of (S)-1,1'-binaphthyl-2,2'-diol, 4,4'-sulfonyl diphenol and 4,4'-difluoro benzophenone,

and (ii) subsequent sulfonation of the resulting polymers using ClSO_3H . The chemical structures were confirmed by 2D ^1H - ^1H COSY NMR and FT-IR. The conjugated but non-coplanar structure of binaphthyl unit endorsed excellent solubility and film-forming properties to the SPAEKs. By tuning the loading amount of (S)-1,1'-binaphthyl-2,2'-diol, three SPAEKs with IECs ranging from 1.40 to 1.89 mmol g^{-1} were obtained. The SPAEK-50 with an IEC of 1.89 $\text{mmol}\cdot\text{g}^{-1}$ exhibited a proton conductivity of 102 mS cm^{-1} at 30 °C, much higher than that of the state-of-the-art Nafion N212 membrane and those of many previously reported aromatic analogs, which may be attributed to the likely large intrinsic free volume of SPAEKs created by the highly twisted chain structures and the desirable microscopic morphology. Along with the remarkable thermal stabilities, oxidative stabilities, and mechanical properties, the SPAEKs were demonstrated to be promising PEM candidates for potential membrane separations.

Author Contributions: Conceptualization, W.Z. and D.C.; Methodology, W.Z. and Z.Y.; Investigation, W.Z., Z.Y. and S.C.; Writing-Original Draft Preparation, W.Z. and Z.Y.; Writing-Review & Editing, D.C.; Supervision, D.C.; Project Administration, D.C.; Funding Acquisition, D.C.

Funding: This work was supported by the National Natural Science Foundation of China (Grant Numbers: 51,873,037 and 51503038) and Natural Science Foundation of Fujian Province (Grant Number: 2015J05030).

Conflicts of Interest: The authors declare no conflict of interest.

References

1. Vallejo, E.; Pourcelly, G.; Gavach, C.; Mercier, R.; Pineri, M. Sulfonated polyimides as proton conductor exchange membranes. Physicochemical properties and separation H^+/Mz^+ by electro dialysis comparison with a perfluorosulfonic membrane. *J. Membr. Sci.* **1999**, *160*, 127–137. [[CrossRef](#)]
2. Wang, Q.Z.; Lu, Y.Y.; Li, N. Preparation, characterization and performance of sulfonated poly(styrene-ethylene/butylene-styrene) block copolymer membranes for water desalination by pervaporation. *Desalination* **2016**, *390*, 33–46. [[CrossRef](#)]
3. Hickner, M.A.; Ghassemi, H.; Kim, Y.S.; Einsla, B.R.; McGrath, J.E. Alternative polymer systems for proton exchange membranes (PEMs). *Chem. Rev.* **2004**, *104*, 4587–4611. [[CrossRef](#)] [[PubMed](#)]
4. Li, X.F.; Zhang, H.M.; Mai, Z.S.; Zhang, H.Z.; Vankelecom, I. Ion exchange membranes for vanadium redox flow battery (VRB) applications. *Energy Environ. Sci.* **2011**, *4*, 1147–1160. [[CrossRef](#)]
5. Zhang, H.W.; Shen, P.K. Recent development of polymer electrolyte membranes for fuel cells. *Chem. Rev.* **2012**, *112*, 2780–2832. [[CrossRef](#)] [[PubMed](#)]
6. Zhang, J.; Chen, F.; Ma, X.Y.; Guan, X.H.; Chen, D.Y.; Hickner, M.A. Sulfonated polymers containing polyhedral oligomeric silsesquioxane (POSS) core for high performance proton exchange membranes. *Int. J. Hydrogen Energy* **2015**, *40*, 7135–7143. [[CrossRef](#)]
7. Aviles-Barreto, S.L.; Suleiman, L.D. Suleiman, Transport properties of sulfonated poly(styrene-isobutylene-styrene) membranes with counter-ion substitution. *J. Appl. Polym. Sci.* **2013**, *129*, 2294–2304. [[CrossRef](#)]
8. Benavides, R.; Rodriguez, J.C.O.; Melo, L.; Morales-Acosta, D.; Paula, M.M.S.; da Silva, L. Electrochemical comparison of two sulfonated styrene PEM membranes synthesized by different methods. *J. Appl. Electrochem.* **2015**, *45*, 1211–1215. [[CrossRef](#)]
9. Gao, Y.; Robertson, G.P.; Guiver, M.D.; Mikhailenko, S.D.; Li, X.; Kaliaguine, S. Synthesis of poly(arylene ether ether ketone ketone) copolymers containing pendant sulfonic acid groups bonded to naphthalene as proton exchange membrane materials. *Macromolecules* **2004**, *37*, 6748–6754. [[CrossRef](#)]
10. Guan, R.; Zou, H.; Lu, D.; Gong, C.; Liu, Y. Polyethersulfone sulfonated by chlorosulfonic acid and its membrane characteristics. *Eur. Polym. J.* **2005**, *41*, 1554–1560. [[CrossRef](#)]
11. Wang, L.; Li, K.; Zhu, G.; Li, J. Preparation and properties of highly branched sulfonated poly(ether ether ketone)s doped with antioxidant 1010 as proton exchange membranes. *J. Membr. Sci.* **2011**, *379*, 440–448. [[CrossRef](#)]
12. Li, G.B.; Zhao, C.J.; Li, X.F.; Qi, D.; Liu, C.; Bu, F.Z.; Na, H. Novel side-chain-type sulfonated diphenyl-based poly(arylene ether sulfone)s with a hydrogen-bonded network as proton exchange membranes. *Polym. Chem.* **2015**, *6*, 5911–5920. [[CrossRef](#)]

13. Gui, L.; Zhang, C.; Kang, S.; Tan, N.; Xiao, G.; Yan, D. Synthesis and properties of hexafluoroisopropylidene-containing sulfonated poly(arylene thioether phosphine oxide)s for proton exchange membranes. *Int. J. Hydrogen Energy* **2010**, *35*, 2436–2445. [[CrossRef](#)]
14. Chen, D.; Wang, S.; Xiao, M.; Meng, Y. Synthesis and characterization of novel sulfonated poly(arylene thioether) ionomers for vanadium redox flow battery applications. *Energy Environ. Sci.* **2010**, *3*, 622–628. [[CrossRef](#)]
15. Chang, Y.; Lee, Y.-B.; Bae, C. Partially fluorinated sulfonated poly(ether amide) fuel cell membranes: influence of chemical structure on membrane properties. *Polymers* **2011**, *3*, 222–235. [[CrossRef](#)]
16. Li, N.W.; Cui, Z.M.; Zhang, S.B.; Xing, X. Sulfonated polyimides bearing benzimidazole groups for proton exchange membranes. *Polymer* **2007**, *48*, 7255–7263. [[CrossRef](#)]
17. Ma, L.Y.; Xu, G.X.; Li, S.; Ma, J.; Li, J.; Cai, W.W. Design and optimization of a hyper-branched polyimide proton exchange membrane with ultra-high methanol-permeation resistivity for direct methanol fuel cells applications. *Polymers* **2018**, *10*, 1175. [[CrossRef](#)]
18. Cui, M.B.; Zhang, Z.H.; Yuan, T.; Yang, H.; Wu, L.; Bakangura, E.; Xu, T.W. Proton-conducting membranes based on side-chain-type sulfonated poly(ether ketone/ether benzimidazole)s via one-pot condensation. *J. Membr. Sci.* **2014**, *465*, 100–106. [[CrossRef](#)]
19. Jin, L.; Li, Z.; Wang, S.; Wang, Z.; Dong, F.; Yin, X. Highly conductive proton exchange membranes based on sulfonated poly(phthalazinone ether sulfone) and cerium sulfophenyl phosphate. *React. Funct. Polym.* **2012**, *72*, 549–555. [[CrossRef](#)]
20. Chen, L.; Zhang, S.H.; Jiang, Y.W.; Jian, X.G. Preparation and characterization of sulfonated poly(aryl ether ketone)s containing 3,5-diphenyl phthalazinone moieties for proton exchange membrane. *RSC Adv.* **2016**, *6*, 75328–75335. [[CrossRef](#)]
21. Oh, K.; Ketpang, K.; Kim, H.; Shanmugam, S. Synthesis of sulfonated poly(arylene ether ketone) block copolymers for proton exchange membrane fuel cells. *J. Membr. Sci.* **2016**, *507*, 135–142. [[CrossRef](#)]
22. Nielsen, M.M.; Yang, A.C.C.; Jankova, K.; Hvilsted, S.; Holdcroft, S. Enhancing the phase segregation and connectivity of hydrophilic channels by blending highly sulfonated graft copolymers with fluororous homopolymers. *J. Mater. Chem. A* **2016**, *1*, 8118–8126. [[CrossRef](#)]
23. Yuk, J.; Lee, S.; Nugraha, A.F.; Lee, H.; Park, S.H.; Yi, S.D.; Bae, B. Synthesis and characterization of multi-block poly(arylene ether sulfone) membranes with highly sulfonated blocks for use in polymer electrolyte membrane fuel cells. *J. Membr. Sci.* **2016**, *518*, 50–59. [[CrossRef](#)]
24. Sheng, L.; Higashihara, T.; Zakazawa, S.; Ueda, M. Polystyrenes containing flexible alkylsulfonated side chains as a proton exchange membrane for fuel cell application. *Polym. Chem.* **2012**, *3*, 3289–3295. [[CrossRef](#)]
25. Shang, X.; Fang, S.; Meng, Y. Synthesis and characterization of poly(arylene ether ketone) with sulfonated fluorene pendants for proton exchange membrane. *J. Membr. Sci.* **2007**, *297*, 90–97. [[CrossRef](#)]
26. Chang, Y.; Brunello, G.F.; Fuller, J.; Disabb-Miller, M.L.; Hawley, M.E.; Kim, Y.S.; Hickner, M.A.; Jang, S.S.; Bae, C. Polymer electrolyte membranes based on poly(arylene ether sulfone) with pendant perfluorosulfonic acid. *Polym. Chem.* **2013**, *4*, 272–281. [[CrossRef](#)]
27. Lee, S.W.; Chen, J.C.; Wu, J.A.; Chen, K.H. Synthesis and properties of poly(ether sulfone)s with clustered sulfonic groups for PEMFC applications under various relative humidity. *ACS Appl. Mater. Interfaces* **2017**, *9*, 9805–9814. [[CrossRef](#)] [[PubMed](#)]
28. Takamuku, S.; Jannasch, P. Multiblock copolymers with highly sulfonated blocks containing di- and tetrasulfonated arylene sulfone segments for proton exchange membrane fuel cell applications. *Adv. Energy Mater.* **2012**, *2*, 129–140. [[CrossRef](#)]
29. Chen, G.; Pei, X.; Wei, H.; Xu, L.; Fang, X. Synthesis and characterization of sulfonated block copolyimides derived from 4,4'-sulfide-bis(naphthalic anhydride) for proton exchange membranes. *J. Appl. Polym. Sci.* **2015**, *132*, 41501. [[CrossRef](#)]
30. Matsumoto, K.; Higashihara, T.; Ueda, M. Locally and densely sulfonated poly(ether sulfone)s as proton exchange membrane. *Macromolecules* **2009**, *42*, 1161–1166. [[CrossRef](#)]
31. Chen, D.; Wang, S.; Xiao, M.; Meng, Y.; Hay, A. Novel polyaromatic ionomers with large hydrophilic domain and long hydrophobic chain targeting at highly proton conductive and stable membranes. *J. Mater. Chem.* **2011**, *21*, 12068–12077. [[CrossRef](#)]

32. Matsumura, S.; Hlil, A.R.; Lepiller, C.; Gaudet, J.; Guay, D.; Hay, A.S. Ionomers for proton exchange membrane fuel cells with sulfonic acid groups on the end groups: Novel linear aromatic poly(sulfide-ketone)s. *Macromolecules* **2008**, *41*, 277–280. [[CrossRef](#)]
33. Bae, B.; Miyatake, K.; Watanabe, M. Sulfonated poly(arylene ether sulfone ketone) multiblock copolymers with highly sulfonated block. Synthesis and properties. *Macromolecules* **2010**, *43*, 2684–2691. [[CrossRef](#)]
34. Tian, M.; Pang, Z.B.; Li, H.F.; Wang, L.L. Novel MOP-type H-8-binaphthyl monodentate phosphite ligands and their applications in transition metal-catalyzed asymmetric 1,4-conjugate additions and hydroformylations. *Tetrahedron Asymmetry* **2017**, *28*, 330–337. [[CrossRef](#)]
35. Xu, Q.; Gu, P.; Jiang, H.C.; Wei, Y.; Shi, M. Chiral bidentate NHC ligands based on the 1,1'-binaphthyl scaffold: Synthesis and application in transition-metal-catalyzed asymmetric reactions. *Chem. Rec.* **2016**, *16*, 2740–2753. [[CrossRef](#)] [[PubMed](#)]
36. Chen, D.; Wang, S.; Xiao, M.; Meng, Y. Synthesis and properties of novel sulfonated poly(arylene ether sulfone) ionomers for vanadium redox flow battery. *Energy Convers. Manag.* **2010**, *51*, 2816–2824. [[CrossRef](#)]
37. Yu, G.; Liu, C.; Wang, J.; Li, G.; Han, Y.; Jian, X. Synthesis, characterization, and crosslinking of soluble cyano-containing poly(arylene ether)s bearing phthalazinone moiety. *Polymer* **2010**, *51*, 100–109. [[CrossRef](#)]
38. Chen, D.; Wang, S.; Xiao, M.; Han, D.; Meng, Y. Synthesis of sulfonated poly(fluorenyl ether thioether ketone)s with bulky-block structure and its application in vanadium redox flow battery. *Polymer* **2011**, *52*, 5312–5319. [[CrossRef](#)]
39. He, G.; Li, Z.; Zhao, J.; Wang, S.; Wu, H.; Guiver, M.D.; Jiang, Z. Nanostructured ion exchange membranes for fuel cells: recent advances and perspectives. *Adv. Mater.* **2015**, *27*, 5280–5295. [[CrossRef](#)] [[PubMed](#)]
40. Moh, L.C.H.; Goods, J.B.; Kim, Y.; Swager, T.M. Free volume enhanced proton exchange membranes from sulfonated triptycene poly(ether ketone). *J. Membr. Sci.* **2018**, *549*, 236–243. [[CrossRef](#)]
41. Chen, X.; Lü, H.; Lin, Q.; Zhang, X.; Chen, D.; Zheng, Y. Partially fluorinated poly(arylene ether)s bearing long alkyl sulfonate side chains for stable and highly conductive proton exchange membranes. *J. Membr. Sci.* **2018**, *549*, 12–22. [[CrossRef](#)]
42. Chen, D.; Hickner, M.A. Ion clustering in quaternary ammonium functionalized benzylmethyl containing poly(arylene ether ketone)s. *Macromolecules* **2013**, *46*, 9270–9278. [[CrossRef](#)]



© 2018 by the authors. Licensee MDPI, Basel, Switzerland. This article is an open access article distributed under the terms and conditions of the Creative Commons Attribution (CC BY) license (<http://creativecommons.org/licenses/by/4.0/>).